Galactic kinematics and structure defined by open clusters *

Zi Zhu

Department of Astronomy, Nanjing University, Nanjing 210093, China; *zhuzi@nju.edu.cn*

Abstract On the basis of recently published astrophysical parameters of the open clusters, we have selected 301 clusters with measurements of their kinematical parameters to trace the local structure and kinematics of the Galactic disk. The present sample covers a range of over 3.0 kpc from the Sun and gives significant estimates of the disk structure and kinematical parameters of the Galaxy. We derive the disk scale height, vertical displacement of the Sun to the Galactic plane, solar motion with respect to the local standard of rest, circular speed of the Galactic rotation, Galactocentric distance from the Sun, etc. We found that the average scale height of the disk defined by the open clusters is $z_h = 58 \pm 4$ pc, with a vertical displacement of the Sun below the Galactic plane of $z_0 = -16 \pm 4$ pc. Clusters with ages older than 50 Myr are less concentrated in the average plane ($z_h = 67 \pm 6$ pc) than the younger clusters ($z_h = 51 \pm 5$ pc). Using the approximation of axisymmetric circular rotation, we have derived the distance to the Galactic center from the Sun $R_0 = 8.03 \pm 0.70$ kpc, which is in excellent agreement with the best estimate of the Galactocentric distance. From a kinematical analysis, we found an age-dependent rotation of the Galaxy. The older clusters exhibit a lower velocity of vorticity, but have the same shear as the younger clusters. The mean rotation velocity of the Galaxy was obtained as 235 ± 10 km s^{-1}.

Key words: Galaxy: disk — Galaxy: kinematics and dynamics — Galaxy: open clusters and associations: general — Galaxy: structure

1 INTRODUCTION

Open clusters are considered to be excellent tracers of Galactic structure, kinematics and dynamics in the solar neighborhood. They provide crucial information and constraints for understanding stellar formation and evolution, the structures of the Galactic disks and spiral arms, the gravitational potential of the Milky Way, and the global shape of the Galaxy. Since we believe that star formation in an open cluster takes place nearly simultaneously in the same interstellar cloud, a statistical average should give a more precise measurement of its physical parameters, including its distance, space motion, age, reddening, etc.

Based on various observations, astrophysical parameters for almost 2000 open clusters are available from the literature, in the catalog of open clusters compiled by Lyngå (1987), the database WEBDA developed by Mermilliod and further maintained by Paunzen [1], and the new catalog of optically visible open clusters and candidates (Dias et al. 2002). Recently, Kharchenko et al. (2005a) identified 520 Galactic open clusters and compact associations using a homogeneous method and algorithms that were

[1] *http://www.univie.ac.at/webda//*

based on the astrometric and photometric data from the All-Sky Compiled Catalog of 2.5 million stars (ASCC-2.5, Kharchenko 2001). Subsequently, an additional list of 130 candidate open clusters was published by Kharchenko et al. (2005b), in which 109 clusters were newly discovered. All 650 clusters with their associated parameters were listed in two data sets: the Catalog Open Cluster Data and its Extension 1 (COCD). Using the 2nd version of the Catalog of Radial Velocities with Astrometric Data (CRVAD-2), the mean radial velocities of the open clusters and stellar associations have been newly revised by Kharchenko et al. (2007). Moreover, an updated version of the cluster data was recently given by Dias et al. (2006, 2008).

Thanks to the increase of available data on open clusters, comprehensive studies of the Galactic cluster population have been made by many authors in the recent years. From the kinematical data of the young open clusters, Dias & Lépine (2005) found that most open clusters are formed in the spiral arms, and confirmed the rigid rotation of the spiral arms as predicted by the classical theory of spiral waves. Using COCD data within heliocentric distances less than 0.85 kpc, Piskunov et al. (2006) performed an extensive study of the geometric shape of the Galactic thin disk, and the kinematical and dynamical structure of the Galaxy. They also studied the possible complexes consisting of clusters that are kinematically bound, as well as the formation rate of clusters. Note that in this work it was assumed that the observation of open clusters is complete up to 0.85 kpc from the Sun. A more detailed work about the spatial distribution of the open clusters in the Galactic thin disk was given by Bonatto et al. (2006). They found that the scale height of the disk characterized by the open clusters is strongly dependent on the ages, and increases with the Galactocentric distance.

In our present study, we concentrate on an extensive study of the structure, kinematics and dynamics of the local disk on the basis of the proper-motion and radial velocity data of the open clusters. We reexamine the vertical distribution to derive the local kinematical parameters of the Galaxy and estimate the distance to the Galactic center from the Sun.

2 DATA SELECTION

Our goal in the data selection is to find all clusters with complete space velocity components. The data are based on two catalogs: the COCD compiled by Kharchenko et al. (2005a,b) containing 520+130 clusters, and the earlier updated version of the new catalog of optically visible open clusters and candidates compiled by Dias, Alessi, Moitinho & Lépine (hereafter referred to as DAML02) in which 1689 clusters were collected from the literature (Dias et al. 2002, 2006).

To avoid possible systematic deviations of the physical parameters determined by different investigators, we decided to accept all parameters from COCD if available. Carrying out cross identification, we found 370 clusters supplied with measurements of heliocentric distance, mean proper motions, mean radial velocities, ages, etc., in which 253 clusters were directly found from the list of 520 COCD clusters, 69 were from the COCD extension, and 19 clusters were from DAML02 that are not contained in COCD. In addition, for 29 COCD clusters, the radial velocities were taken from DAML02. For the second part of COCD, we have checked the kinematical data, and found that the clusters exhibit inconsistent kinematical properties with the first part of 520 clusters; thus, we excluded them from further study in the future, leaving a total of 301 clusters with complete spatial velocity measurements for this study.

To examine the possible differences of the spatial distribution and kinematics of the clusters as a function of their ages, we divided all the clusters into two groups: the younger clusters with ages less than 50 Myr (corresponding to $\log t \leq 7.7$), and the older group with ages larger than 50 Myr. Open clusters younger than 50 Myr can clearly trace the structure of spiral arms, including the local arm, and the inner and outer arms, while the spiral structures become too blurred to trace clusters older than that age (Bonatto et al. 2006). Both subsamples are of almost equal size. Figure 1 displays 301 clusters on the Galactic plane. The X-axis is pointing towards the Galactic center, while the Y-axis is towards the direction of Galactic rotation. Clusters with ages younger than 50 Myr are marked by solid dots, while the grey circles represent the clusters older than 50 Myr. The younger clusters in the inner part of the solar circle clearly delineate a logarithmic spiral of the Sagittarius-Carina arm, while the Perseus and
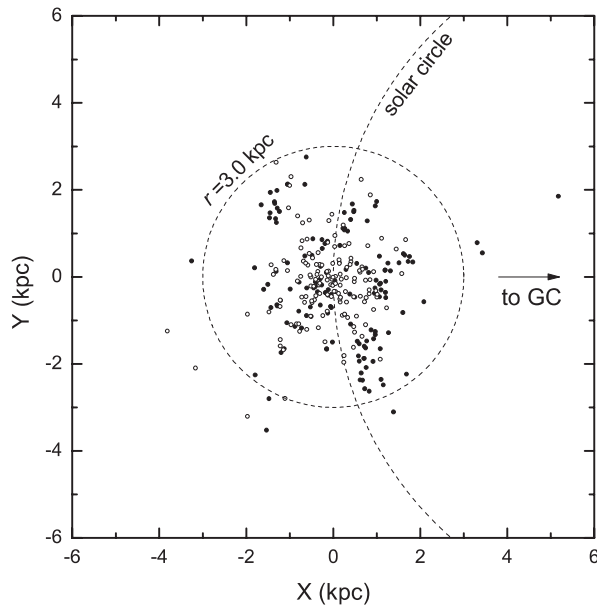
Fig. 1 301 Open clusters distributed on the Galactic plane. The bold dots indicate clusters younger than 50 Myr, and the open circles represent clusters older than 50 Myr.
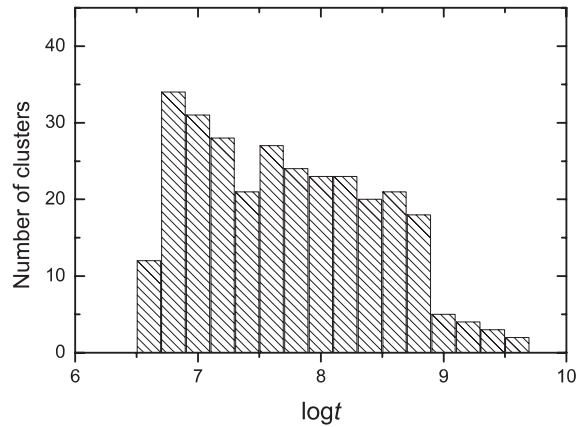
Fig. 2 Age histogram of 301 open clusters. The logarithm of ages ranges roughly from 6.6 to 9.0, corresponding to 4 Myr $\sim$ 1 Gyr.

Orion-Cygnus arms are characterized by the younger clusters which are exterior to the solar circle or near the solar circle. It is shown that most clusters are located within a heliocentric distance $r \leq 3.0$ kpc, and only 18 clusters are more distant than 3.0 kpc.

The age range of most clusters is 4 Myr $\sim$ 1 Gyr, which corresponds to $\log t = 6.6$ to 9.0. Figure 2 shows the age histogram of the present sample of the open clusters.

The velocity data are used to study the peculiar motions of the individual clusters. The components of peculiar motion are derived from the first order expansion of an asymmetric rotation of the systematic

velocity field:

$$
\begin{aligned}
\kappa r \Delta \mu_\ell \cos b = {} & \kappa r \mu_\ell^{\mathrm{obs}} \cos b - A r \cos 2\ell \cos b - B r \cos b \\
& + C r \sin 2\ell \cos b - U_\odot \sin \ell + V_\odot \cos \ell \,, \quad (1)
\end{aligned}
$$

$$
\begin{aligned}
\kappa r \Delta \mu_{\mathrm{b}} = {} & \kappa r \mu_{\mathrm{b}}^{\mathrm{obs}} + A r \sin 2\ell \sin b \cos b \\
& + C r \cos 2\ell \sin b \cos b + K r \sin b \cos b \,, \\
& - U_\odot \cos \ell \sin b - V_\odot \sin \ell \sin b + W_\odot \cos b, \quad (2)
\end{aligned}
$$

$$
\begin{aligned}
\Delta v_{\mathrm{r}} = {} & v_{\mathrm{r}}^{\mathrm{obs}} - A r \sin 2\ell \cos^2 b \\
& - C r \cos 2\ell \cos^2 b - K r \cos^2 b \\
& + U_\odot \cos \ell \cos b + V_\odot \sin \ell \cos b + W_\odot \sin b \,, \quad (3)
\end{aligned}
$$

where r is the heliocentric distance of a cluster in kpc, $v_{\mathrm{r}}^{\mathrm{obs}}$, μ_ℓ^{obs} and $\mu_{\mathrm{b}}^{\mathrm{obs}}$ are the observed radial velocity in $\mathrm{km\,s^{-1}}$ and the proper motion in $\mathrm{mas\,yr^{-1}}$ of a cluster. The Oort constants A, B, C and K are in units of $\mathrm{km\,s^{-1}\,kpc^{-1}}$, and $U_\odot$, $V_\odot$ and $W_\odot$ are the components of the solar motion in $\mathrm{km\,s^{-1}}$ with respect to the LSR. The detailed description of the solar motion and the Oort constants will be given in Section 4. The constant κ is equal to 4.47047. Deviations of $\Delta \mu_\ell$, $\Delta \mu_{\mathrm{b}}$ and Δv_{r} are the proper motion and radial velocity differences from the kinematical model and the observed quantity for a given cluster.

Accepting Oort's constants and the components of the solar motion listed in Table 5 from the all age cluster solution, the velocity of the peculiar motion for the individual cluster is obtained. Clusters with peculiar velocities larger than $50\,\mathrm{km\,s^{-1}}$ (roughly 2.6σ of the total velocity dispersion, see Sect. 4) are shown in Table 1, where z is the vertical component of the Galactic coordinates of a cluster, and Δv is its random motion related to the LSR. It is shown that we have detected 22 clusters from 301 samples with random velocities larger than $50\,\mathrm{km\,s^{-1}}$, and among them 12 clusters actually have heliocentric distances larger than 3 kpc. Figure 3 shows the distribution of the determined Δv for the 301 clusters. 269 clusters in the dotted rectangle ($\Delta v \leq 50\,\mathrm{km\,s^{-1}}$ and $r \leq 3.0\,\mathrm{kpc}$) will be selected for the kinematical analysis in Section 4.

Table 1 Clusters with Random Motions Larger than $50\,\mathrm{km\,s^{-1}}$

	Name of OC	r (kpc)	z (kpc)	$\Delta v\,(\mathrm{km\,s^{-1}})$
1	NGC 1664	1.20	–0.01	50.38
2	NGC 2354	3.79	–0.45	114.15
3	Haffner 16	3.17	0.03	64.95
4	NGC 2506	3.46	0.60	61.69
5	Ruprecht 47	3.01	–0.01	78.60
6	NGC 2527	0.60	0.02	113.10
7	Ruprecht 55	4.89	0.07	95.13
8	Ruprecht 79	1.98	–0.03	60.74
9	Trumpler 16	2.84	–0.03	69.54
10	Bochum 12	2.22	–0.07	61.65
11	Pismis 17	3.50	0.01	101.22
12	Ruprecht 94	3.40	–0.12	53.61
13	Ruprecht 141	5.50	–0.12	57.74
14	NGC 6705	1.88	–0.09	64.83
15	Ruprecht 147	0.18	–0.04	54.62
16	NGC 7789	2.34	–0.22	71.61
17	vdBergh 1	1.69	–0.05	54.53
18	Dolidze 25	6.30	–0.14	116.72
19	Berkeley 31	8.27	0.74	223.96
20	NGC 2324	3.81	0.22	68.67
21	Lynga 6	1.60	0.01	95.64
22	NGC 6791	5.85	1.11	121.71
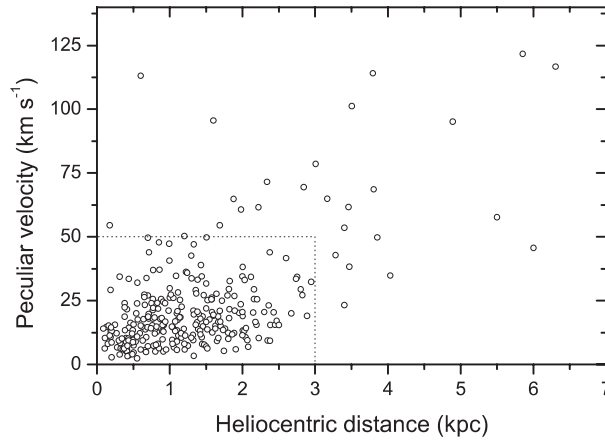
Fig. 3 Distribution of the peculiar velocities determined for 301 open clusters. Among them, there are 283 clusters with heliocentric distances of less than 3.0 kpc, and 269 clusters are located in the dotted rectangle with velocity dispersions less than 50 km s^{-1}.

Table 2 Clusters with Galactic Height $|z|$ Larger than 0.3 kpc

	Name of OC	r (kpc)	z (kpc)	Δv(km s^{-1})
1	NGC 2354	3.79	−0.45	114.15
2	NGC 2439	3.86	−0.30	49.86
3	NGC 2506	3.46	0.60	61.69
4	NGC 2682	0.91	0.48	24.58
5	NGC 188	2.05	0.78	14.33
6	NGC 2141	4.03	−0.41	34.86
7	Berkeley 31	8.27	0.74	223.96
8	NGC 2355	2.20	0.45	25.52
9	NGC 6791	5.85	1.11	121.71
10	NGC 6819	2.36	0.35	23.18

The measured random motion Δv is composed of the velocity dispersion, the measurement errors in the radial velocity, heliocentric distance and proper motion, and possible errors from the model. It is reasonable to believe that the measurement errors in radial velocity and in proper motion are known to a few km s^{-1} or mas yr^{-1}. It is well known that the rotation curve of the Galaxy is nearly flat with a small decline which accounts for a wide range from the Sun; thus modeling errors for Δv should be small in comparison with 50 km s^{-1}. Therefore, the measured large random motions should mainly represent both the velocity dispersion of a cluster and the large measurement error of the heliocentric distance. The average velocity dispersion for the open cluster population is less than 20 km s^{-1} (Piskunov et al. 2006), thus, for the distant clusters with extremely large Δv listed in Table 1, the determined random motions should be dominated by the distance calibration. In fact, the calibration of the photometric distances of clusters depends on the total extinction. For the distant clusters, the calibration of their heliocentric distances is very difficult.

The uncertainty of the distance estimate directly affects the measurement of the z component of the Galactic coordinates. From 301 clusters, we found 10 clusters with a Galactic height $|z|$ larger than 300 pc; among them 6 clusters are removed because they have heliocentric distances larger than 3.0 kpc and large random motions (Table 2).

From the discussion above, we conclude that the precision of the distance calibration might be problematic for the distant clusters. In order to avoid such problems, we simply confine ourselves to be

within the range of $r \leq 3.0$ kpc for the following investigation, in which case the adopted sample of clusters is only 283.

3 GEOMETRIC DISTRIBUTION PERPENDICULAR TO THE GALACTIC PLANE

One generally assumes that the formation of the thin disk represents the final stage in the dissipative settling of the disk gas. The spatial distribution of the open clusters characterizes the local structure of the thin disk of the Galaxy. The vertical density and motions of the clusters provide a direct constraint for evaluating the local mass density of our Galaxy. Oort first obtained the volume density near the Sun ρ_0 (Oort 1932), called the Oort limit in his honor, which was estimated from the density distribution of several stellar populations. Recently, there have been many investigations into the vertical structure and distribution of the Galactic disk based on different observations, including star counts from SDSS data by Chen et al. (2001), from the Hipparcos observations by Kaempf et al. (2005), and from the astrometric data of the Second Guide Star Catalog (GSC-II) by Spagna et al. (2005). More recent studies of the structure and distribution of the Galactic open clusters were made by Piskunov et al. (2006), and by Bonatto et al. (2006). In this Section, we will extend the study of the vertical structure of the open clusters.

The local vertical distribution of stars is usually expressed as an exponential-decay function: $\phi(z) = \phi_0 e^{-|z-z_0|/z_{\mathrm{h}}}$, where z_0 is the position of the Galactic symmetry plane, z_{h} is the scale height of the distribution, and ϕ_0 is the density at z_0. Note that ϕ_0 is not an independent parameter. If N^* is the total number of clusters, then,

$$\phi(z) = \frac{N^*}{2z_{\mathrm{h}}} e^{-|z-z_0|/z_{\mathrm{h}}} \ . \tag{4}$$

It can be seen that the density ϕ_0 is only meaningfully determined if the sample is spatially complete. In the last section, we have selected all those clusters with associated radial-velocity and proper-motion measurements, without any consideration of the sample incompleteness. Thus, the selected sample probably cannot characterize the real distribution of the disk. However, it is easy to understand that the randomly selected sample does not change the form of the distribution of the exponential decay, as long as these clusters are an unbiased subset randomly selected from the complete sample of clusters. This implies that the distribution function defined by the present sample will result in a fictitious density ϕ_0, while z_0 and z_{h} cannot be significantly affected. Thus, we will only refer to the last two parameters in the following discussion.

The vertical distribution of clusters within a heliocentric distance of $r \leq 3.0$ kpc is illustrated in Figure 4. In order to study the properties of the clusters in different age ranges, we divide the clusters into two subsets: 142 younger clusters with an age less than 50 Myr, and 141 older clusters with an age larger than 50 Myr.

The distribution profiles are fitted in Figure 4 for the two subsets of clusters (middle and bottom panels) and for all clusters (top panel), while the results are given in Table 3. In our analysis, we have adopted different size bins to check the estimated parameters. We found that the selected bin size does not change our determination of the distribution parameters significantly, as long as the sample size is sufficient to be fit by the model. For comparison, we list solutions from the distribution profiles in bins of 10 pc and in bins of 20 pc, respectively. This shows that neither z_0 nor z_{h} have been meaningfully changed with the change of bin-size. This fact is easily explained, since the total observed errors are not changed with the bin-size.

Comparing solutions for the younger clusters and for the older clusters, we found that both z_0 and z_{h} depend on the age of clusters, while the values of z_0 and/or z_{h} from all clusters are approximately equal to the average of those derived from the younger and older subsets of clusters. Considering the estimated errors of the parameters, the displacement of the Galactic plane with respect to the Sun, derived from the younger and older clusters, is not significantly different. However, for z_{h}, the scale height is remarkably varied with the age of the clusters. Thus, we need to discuss the real character of the distribution in more detail.
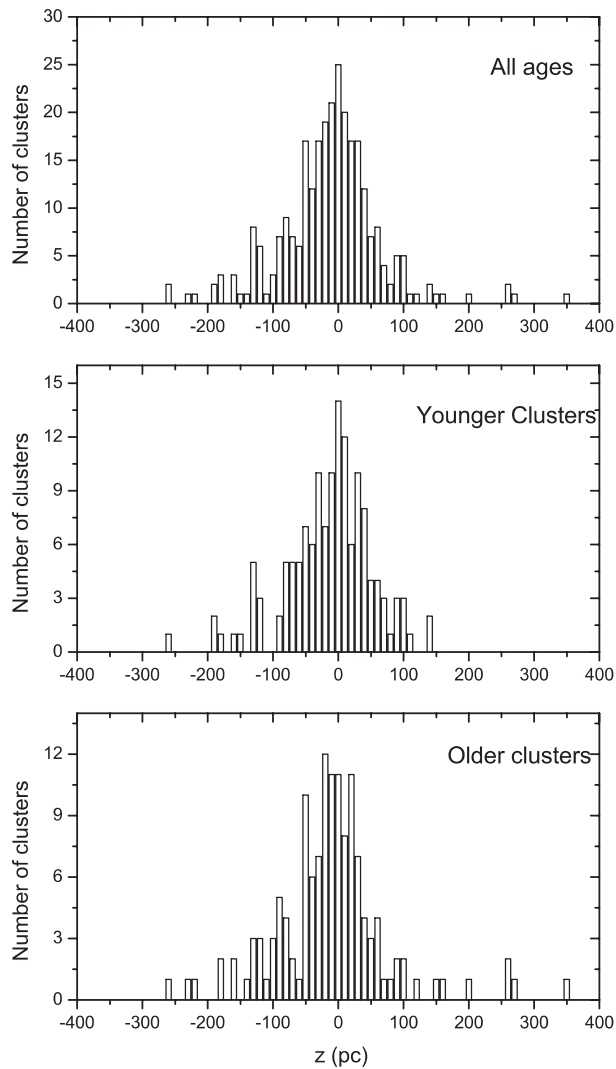
Fig. 4 Distribution histogram of clusters perpendicular to the Galactic plane in bins of 10 pc. The upper panel gives all 283 clusters within $r \leq 3.0$ kpc. 142 clusters younger than 50 Myr are shown in the middle panel. The bottom panel represents the distribution of 141 clusters older than 50 Myr.

3.1 Clusters Embedded in Gould's Belt

It was recognized long ago that Gould's Belt is a local subsystem of early type stars associated with substantial amounts of expanding interstellar gas and dust. It is mainly composed of O-A type stars younger than $30 - 40$ Myr (Westin 1985; Lindblad 2000). This system extends from about –600 pc to 300 pc along the X-axis and has an inclination of about $20°$ to the Galactic plane. Figure 5 shows this distribution of the Hipparcos Gould-Belt O-B stars projected on the X-Z plane. Various young streams are known to be surrounding the expanding Lindblad gas ring, including the Sco-Cen complex and Vel OB2 association (Olano 1982; Torra et al. 2000).

In a kinematical analysis, Piskunov et al. (2006) identified 23 clusters with high membership probability, forming an open cluster complex (OCC) associated with Gould's Belt. In order to investigate

Table 3 Parameter solutions for the vertical distribution. The number of clusters in each sample subset is given in brackets in the first column. In the last 4 lines, we show the results derived by Piskunov et al. (2006) and by Bonatto et al. (2006).

	bins=10 pc		bins=20 pc	
	z_0 (pc)	z_h (pc)	z_0 (pc)	z_h (pc)
all ages (283)	−18.6	63.9	−17.7	62.6
	± 3.8	± 3.8	± 3.5	±3.7
≤ 50 Myr (142)	−15.0	58.1	−14.8	56.4
	± 4.3	± 4.9	± 4.2	±4.7
> 50 Myr (141)	−21.8	70.3	−21.9	70.2
	± 5.2	± 5.9	± 4.7	±5.9
all ages (Piskunov et al. 2006)			−22 ± 4	56 ± 3
all ages (Bonatto et al. 2006)			−14.8 ± 2.4	57.2 ± 2.8
≤ 200 Myr (Bonatto et al. 2006)				47.9 ± 2.8
200 ∼ 1000 Myr (Bonatto et al. 2006)				149.8 ± 26.3
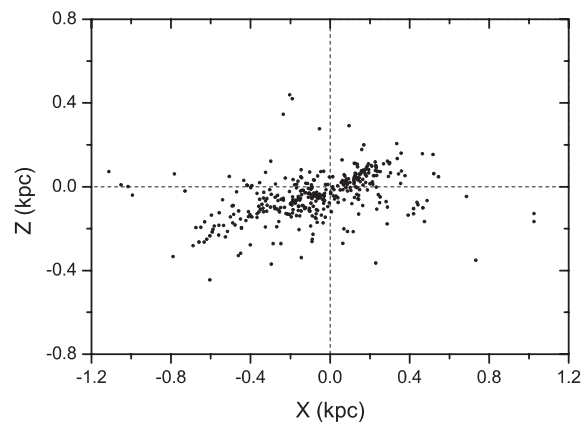
Fig. 5 Distribution of the Gould-Belt O-B stars taken from the Hipparcos Catalog.

the vertical distribution of the Galactic disk, we decided to remove all asymmetrically distributed OCC members from our sample, and we detected a total of 17 clusters in our previous sample that belong to the complex. Figure 6 illustrates the field clusters, among which these 17 members of the OCC are interspersed.

Among the 17 members of the Gould-Belt OCC, there are 13 clusters with an age younger than 50 Myr and 4 clusters older than 50 Myr. Fitting these clusters in Figure 6, we found that the Gould-Belt associations have an inclination of $17.4° ± 2.4°$ to the Galactic plane. Deleting these 17 clusters, we recalculate the parameters z_0 and z_h, and list the results in Table 4.

It is clear that the scale heights tend to decrease when the Gould's-Belt OCC clusters are excluded, especially for the younger clusters with an age less than 50 Myr. The average position of the Galactic plane with respect to the Sun is $z_0 = −16 ± 4$ pc, which is consistent with that determined by Piskunov et al. (2006) or by Bonatto et al. (2006). The mean scale heights are found to be $58 ± 4$ pc for all ages, $51 ± 5$ pc for the younger clusters, and $67 ± 6$ pc for the older sample. Note that the mean age of all clusters is 200 Myr, while the mean ages are 17 Myr for the younger clusters, and 380 Myr for the older clusters. From the above analysis, we conclude that disk height for the younger clusters is significantly less than for the older clusters.
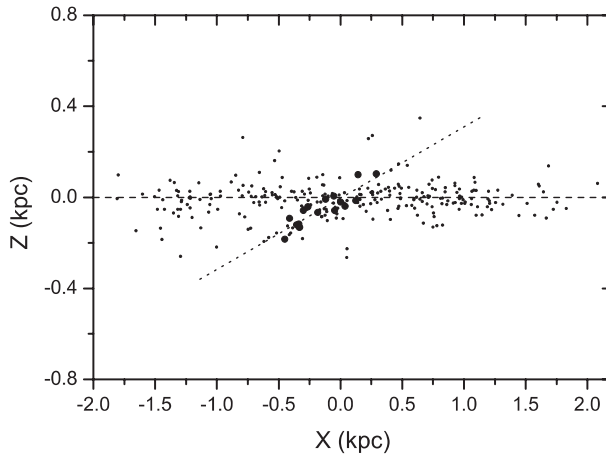
Fig. 6 17 members of the Gould-Belt OCC included in the sample. The field clusters are marked by the small dots, the bold dots represent the members of the OCC. The dotted line fits clusters belonging to the OCC with an inclination of $17.4° \pm 2.4°$ to the Galactic plane.

Table 4 Solution for Parameters of the Vertical Distribution Derived from Clusters the 17 Excluded Members of Gould's-Belt OCC

	bins=10 pc		bins=20 pc	
	z_0 (pc)	z_h (pc)	z_0 (pc)	z_h (pc)
all ages (266)	−16.1	58.3	−15.6	56.8
	± 4.0	± 4.0	± 3.5	± 3.5
≤ 50 Myr (129)	−12.3	51.8	−12.4	49.6
	± 4.2	± 4.6	± 4.2	± 4.4
> 50 Myr (137)	−20.5	67.8	−19.5	67.1
	± 5.6	± 5.8	± 5.7	± 5.7

3.2 Scale Height for the Oldest Clusters

In the last sub-section, we determined the scale heights for three groups of clusters. Comparing our results with that given by Piskunov et al. (2006) and by Bonatto et al. (2006) listed in Table 3, we found that all solutions are mutually consistent except for $z_h \simeq 150$ pc for clusters aged $200 \sim 1000$ Myr given by Bonatto et al. (2006), far from our determination for the older clusters. This discrepancy should be reexamined, even though the age ranges and the selected samples are not entirely identical between ours and those used by Bonatto et al.

In fact, the estimated parameters of z_0 and z_h derived from Equation (4) are strongly dependent on the errors of the observations. In general, the cluster positions are accurate enough for our investigation, due to the highly precise astrometric observations. Thus, the dominant error source contributed to the measurement of the Galactic height z of a cluster is only from the heliocentric distance. This means that the relative errors in z and in r are almost the same for a given cluster. Suppose the relative error is a constant for any cluster, then, the measurement error in z is proportional to r. In practice, the observed relative errors in distance might be more pronounced for the more distant objects, say, the distances derived from the Hipparcos parallaxes. Similarly, clusters with large heliocentric distances should share large errors for the z components. This fact can be examined in the top panel of Figure 7, especially for those clusters removed with $r > 3$ kpc. In Section 2, we have already reported the problematic peculiar motions of clusters with distances larger than 3 kpc which again verifies our present finding. A recent
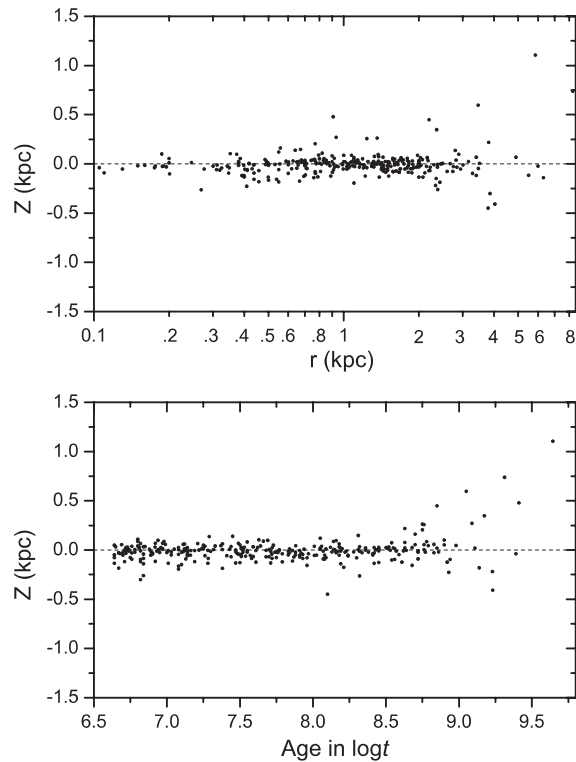
Fig. 7 Vertical distribution of clusters as functions of heliocentric distances r (*upper panel*) and cluster ages (*bottom panel*). Clusters with $r > 3$ kpc exhibit a scattered distribution along the direction perpendicular to the Galactic plane. It may not be an accident that the dispersion increases roughly at age > 8.5 in $\log t$ in the bottom panel.

statistical study of the cluster parameters by Pauzen & Netopil (2006) shows that about 80% of clusters have relative errors in distances less than 20%, as determined from repeated observations of clusters by several published investigations.

When we observe the bottom panel of Figure 7, we might arrive at the conclusion that for clusters with a logarithmic age of > 8.5, the scale height abruptly increases. Obviously, this observation does not have a reasonable explanation based on Galactic dynamics.

On the other hand, the accuracy of the age may be even worse. Pauzen & Netopil (2006) demonstrated that the relative errors in age are not better than 20% for most clusters, while the worst values even exceed 200%. The photometric distance and age depend on the total absorption. Therefore, the estimated distance and age of the clusters may be correlated. In general, the stars observed in a cluster are dimmed and their numbers are decreased by interstellar absorption. It is known that the photometric uncertainty rapidly increases at faint magnitudes, and as a result, that will greatly decrease the accuracy in the observed distance and age. In the bottom panel of Figure 7, we show the vertical distribution of clusters as a function of the age. The scatter increases roughly at age > 8.5 in $\log t$, however, the majority of those clusters have already been removed since they have $r > 3$ kpc.

Due to the lack of estimated errors in the cluster parameters in the literature, any weighting of the observed quantities could be dangerous. A simple way is to delete the problem clusters as before. If not, then clusters with large errors in distances should introduce a remarkable deviation from their real distribution, and an enlarged scale height would be obtained as a consequence. That may be why an extremely large value of $z_h \simeq 150$ pc for clusters older than 200 Myr was derived by Bonatto et al. (2006).

3.3 Scale Height and Measurement Errors in Distances

From the above analysis and discussion, we get some information on the evolution of the disk height based on the cluster age, and knowledge that the measured scale height has been infected by the uncertainty of the distance. In this subsection, we will go further in discussing the statistical property of the errors in distance and their influence on the scale height.

For clusters in the thin disk, the observed Galactic latitudes are generally small with the exception of the nearby clusters. The estimated error in z is therefore approximately proportional to the distance error. Thus, the forms of the error distribution in r and in z are similar.

Suppose the function of the error distribution $e(z)$ is known, and the vertical distribution of clusters can be strictly expressed as the exponential-decay function in Equation (4), then the observed profile of the vertical distribution of clusters is given as $f(z) = e(z) * \phi(z)$, where '$*$' stands for the operator of the convolution integral. Thus, the observed $f(z)$ is the only broadened profile other than $\phi(z)$ itself. Direct fitting to the profile with an exponential-decay function will return an overestimated scale height. The real distribution $\phi(z)$ can only be recovered if the error distribution is known.

Assuming the error distribution is Gaussian, we simulate the observed profile with a known measurement error. Figure 8 shows the estimated scale height derived from an exponential-decay fit to the simulated profile. We set a fixed $z_\mathrm{h} = 50 \, \mathrm{pc}$ and σ_z=10, 20, 30, and 50 pc, respectively. The deviation of the estimated scale height increases steeply at large measurement errors.

We conclude that the scale height derived from observation without considering its error contribution should result in an overestimate of its real value, depending on the error.
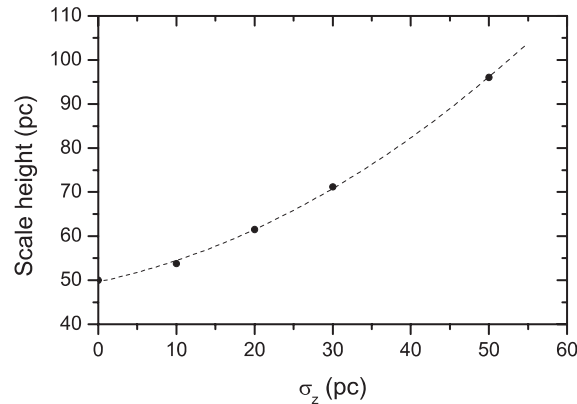
Fig. 8 Simulation of an error dependent scale height derived from a direct exponential-decay fit. The 'real' scale height is fixed to $z_\mathrm{h} = 50 \, \mathrm{pc}$, and a Gaussian error distribution is assumed. Accepting σ_z=10, 20, 30, and 50 pc, respectively, the corresponding estimated scale heights are marked as the thick dots. The dashed curve gives the 2nd order polynomial fit to the dots.

4 GALACTIC KINEMATICS FROM OPEN CLUSTERS

In this section, we will perform a kinematical analysis of the local thin disk defined by the open clusters. In order to describe the velocity field, we employ Galactocentric cylindrical coordinates (R, θ, Z) to express the kinematical parameters. Here, R is measured from the Galactic center and R_0 is the distance to the Galactic center from the Sun. The azimuthal angle is measured counterclockwise to the direction of Galactic rotation, and Z is towards the north Galactic pole. The LSR is defined as V_0, and the Sun moves with a peculiar velocity of $(U_\odot, V_\odot, W_\odot)$ with respect to the LSR. Since the open clusters are confined to the Galactic plane with a small scale height of $\sim$60 pc, a two dimensional asymmetric model

Table 5 Kinematical parameters derived from proper motions and radial velocity. The unit is in $\mathrm{km\,s^{-1}}$ for components of the solar-motion and velocity ellipsoid. The Oort constants are measured in $\mathrm{km\,s^{-1}\,kpc^{-1}}$.

	$U_\odot$	$V_\odot$	$W_\odot$	σ_1	σ_2	σ_3	A	B	C	K
all ages (269)	11.76	13.33	8.11	14.02	11.71	8.75	16.44	−12.91	0.50	−2.60
	±0.59	±0.56	±0.53	±0.74	±0.63	±0.54	±0.94	±0.89	±0.97	±0.93
≤ 50 Myr (137)	10.84	14.62	7.88	13.14	11.08	8.71	16.50	−14.56	2.86	−1.09
	±0.70	±0.67	±0.62	±0.91	±0.75	±0.71	±0.85	±0.83	±0.85	±0.89
> 50 Myr (132)	12.32	12.77	8.18	14.91	12.33	8.78	16.38	−10.93	−2.73	−4.58
	±0.90	±0.83	±0.84	±1.15	±1.01	±0.83	±1.68	±1.61	±1.72	±1.76

should be satisfactory to describe their motions on the Galactic plane. In this case, the Oort constants can be expressed as

$$A = \frac{1}{2}\left(\frac{\partial V_\theta}{\partial R} - \frac{V_\theta}{R} + \frac{1}{R}\frac{\partial V_R}{\partial \theta}\right)_{R=R_0}, \tag{5}$$

$$B = \frac{1}{2}\left(\frac{\partial V_\theta}{\partial R} + \frac{V_\theta}{R} - \frac{1}{R}\frac{\partial V_R}{\partial \theta}\right)_{R=R_0}, \tag{6}$$

$$C = \frac{1}{2}\left(\frac{\partial V_R}{\partial R} - \frac{V_R}{R} - \frac{1}{R}\frac{\partial V_\theta}{\partial \theta}\right)_{R=R_0}, \tag{7}$$

$$K = \frac{1}{2}\left(\frac{\partial V_R}{\partial R} + \frac{V_R}{R} + \frac{1}{R}\frac{\partial V_\theta}{\partial \theta}\right)_{R=R_0}. \tag{8}$$

The parameters A and C denote the azimuthal and radial strain (shear) of the velocity field, B characterizes the vorticity (rotation), and K implies an overall contraction or expansion measured at the Sun. Based on proper motions, radial velocities and heliocentric distances of open clusters, these parameters, including solar motions, can be obtained via a least-squares solution. A detailed description of the kinematical model was given by Zhu (2000).

As we discussed in Sections 2 and 3, the clusters further than 3 kpc have problems with their distances and were removed. Inspecting the peculiar velocities of clusters, few have extremely large random motions. We decided to reject all clusters with random motions larger than $50\,\mathrm{km\,s^{-1}}$ in the following analysis, that is roughly at a 2.6σ level of the total velocity dispersion. Within the domain $(r \leq 3.0\,\mathrm{kpc},\ \Delta v < 50\,\mathrm{km\,s^{-1}})$, we have 269 clusters in total for the kinematical analysis.

Solutions of the solar motion and Oort constants are given in Table 5. Due to the lack of measurement errors in distances, and the rarity of those in radial velocities, we have to use simple fitting errors to calculate the standard deviations for the estimated parameters from our model. In fact, it is difficult to establish a reasonable weighting system because of the complexities arising from the measurement errors and velocity dispersions.

The components of the velocity ellipsoid $(\sigma_1, \sigma_2, \sigma_3)$ are derived from the velocity differences $(\Delta\mu_\ell, \Delta\mu_b, \Delta v_r)$ of clusters as described in Equations (1) – (3), rather than from a simple average with the formula $\sigma_i = \langle (v_i - \langle v_i \rangle)^2 \rangle^{1/2}$.

Comparing solar motions in Table 5 with those given by Dehnen & Binney (1998), who obtained 3 components of solar motion $(10.00 \pm 0.36, 5.25 \pm 0.62, 7.17 \pm 0.38)$ in $\mathrm{km\,s^{-1}}$, we find that X and Z components are successfully determined from the clusters, although ours are a little large. For the second component, we cannot make a direct comparison, because their $V_\odot$ was an extrapolation from the Hipparcos main-sequence stars to a dynamical cold limit. Our 3 components are also a little larger than those given by Piskunov et al. (2006) obtained from proper motions of clusters, but that may be caused by the different sample ranges. Instead of using $r \leq 3$ kpc, they confined their sample to within $r \leq 0.85$ kpc. Using the Hipparcos proper motions of the O-B5 stars within $r \leq 3$ kpc, the determined solar motion in our previous work (Miyamoto & Zhu 1998) is consistent with our present determination.

The velocity dispersion $\sigma = (13.86 \pm 0.81, 8.75 \pm 0.51, 5.50 \pm 0.30)$ in km s^{-1} given by Piskunov et al. seems less than ours. This can be explained by the different sample ranges adopted for the solar motions. When we confine ourselves in $r \leq 0.85$ kpc from the Sun, we obtain $\sigma = (13.36 \pm 1.24, 9.83 \pm 1.03, 5.33 \pm 0.36)$, which is similar to that given by Piskunov et al., but with larger estimated errors due to the smaller number of clusters.

The difference of the velocity dispersions for the younger and for the older clusters is clearly seen, which reflects the dynamical evolution of clusters. The total velocity dispersion for the younger clusters is $\sigma = 19.3 \pm 0.8$ km s^{-1}, while it is $\sigma = 21.2 \pm 1.0$ km s^{-1} for the older clusters.

In an axisymmetric and stationary disk, the Oort constants A and B describe a differential circular rotation of the Galaxy at the Sun. Feast & Whitelock (1997) found a low angular speed ($A = 14.8 \pm 0.8$, $B = -12.4 \pm 0.6$ km s^{-1} kpc^{-1}) from the Hipparcos proper motions of the Galactic Cepheids that is the best approach to the recommended values by IAU 1985 for the Oort constants (Kerr & Lynden-Bell 1986). However, the majority of measurements in recent years show a more or less enhanced angular speed, including our present determination. From the Hipparcos proper motions of the Galactic O-B5 stars, Miyamoto & Zhu (1998) derived $A = 16.1 \pm 1.1$ and $B = -15.6 \pm 0.8$ in km s^{-1} kpc^{-1}. Méndez et al. (1999, 2000) obtained an even higher LSR speed of 270 km s^{-1} based on stellar proper motions from the Southern Proper Motion Program, assuming $R_0 = 8.5$ kpc. From proper motions of the old red giants from the ACT/Tycho-2 catalogs, Olling & Dehnen (2003) found $A - B \simeq 32.8$ km s^{-1} kpc^{-1}. Based on more than 8 years of observations of the massive compact radio source Sgr A* at the Galactic center by the Very Long Baseline Array with respect to the extragalactic sources, Reid & Brunthaler reported the apparent proper motion of Sgr A* $\mu_\ell = -6.379 \pm 0.026$ and $\mu_b = -0.202 \pm 0.019$ mas yr^{-1} (Reid & Brunthaler 2004). This apparent motion should fully reflect the Galactic rotation at the Sun, assuming Sgr A* is at rest. Then we have

$$A - B = -\kappa\mu_\ell - \frac{V_\odot}{R_0}, \tag{9}$$

where $V_\odot = 5.25 \pm 0.62$ km s^{-1} is the component of the solar motion in the direction of Galactic rotation given by Dehnen & Binney (1998). Adopting $R_0 = 8.0$ kpc, we yield $A - B = 29.58 \pm 0.14$ km s^{-1} kpc^{-1}. This is in excellent agreement with our determination from the cluster sample with all ages. The present determination gives a rotation speed of $V_0 = 235 \pm 10$ km s^{-1} from all ages, while it is $V_0 = 248 \pm 9$ km s^{-1} or $V_0 = 218 \pm 19$ km s^{-1} for the younger or older clusters.

Checking the Oort constant A obtained from the younger group of clusters and from the older one, we find that it is unchanged, whereas the absolute value of the Oort constant B decreases with the age. This process of the slowdown of the Oort constant B may arise from the scattering of molecular clouds and from the heating of the irregular gravitational field caused by spiral arms, which lead to the increase of the velocity dispersion as well. A steady shear motion accompanied by a decelerated vorticity of the motion gives us a comprehensible kinematical pattern to trace the origin and evolution of the spiral arms. A recent investigation of the motion of the spiral pattern based on the kinematical data of the younger open clusters was given by Dias & Lépine (2005).

Radial shears with opposite signs are found for the younger and older clusters, but the mean C and K constants derived from all clusters are nearly the same as those given by Torra et al. (2000) from the Hipparcos O-B stars. A persistent negative K term may imply an offset of the zero point of the radial velocity system, or an oval orbit of clusters governed by the elliptic disk-potential. We will discuss in further detail later.

5 DISTANCE TO THE GALACTIC CENTER FROM THE SUN

The determination of the Galactocentric distance of the Sun R_0 is a continuing and fundamentally important task for astronomers. The precision of R_0 is directly related to many astronomical quantities, measurements and theories. Due to the extremely strong obscuration in the central region of the Milky Way, a direct measurement of R_0 is actually impossible. According to the statistical analysis from the individual determinations by Reid (1993), $R_0 = 8.0 \pm 0.5$ kpc is currently considered as the best value,

whereas the 1985 IAU standard value was 8.5 kpc and 1964 IAU adopted $R_0 = 10$ kpc (Kerr & Lynden-Bell 1986). Considerable bias and uncertainty may still exist in the determinations of R_0, even though people have expended many efforts to improve it, e.g. from the latitude proper motion of the Sgr A* source at the Galactic center $\mu_{\rm b} = -0.202 \pm 0.019$ mas yr^{-1} given by Reid & Brunthaler (2004), we yield

$$R_0 = \frac{1}{\kappa} \frac{W_\odot}{\mu_{\rm b}} = 7.49 \pm 0.81 \text{ kpc}, \tag{10}$$

supposing Sgr A* is in rest. Here $W_\odot = 7.17 \pm 0.38$ km s^{-1} is the component of the solar motion taken from Dehnen & Binney (1998).

Basically, there are only 3 techniques or methods of observation used for the evaluation of the Galactocentric distance. One is to use the halo objects, e.g. the globular clusters or the RR Lyrae stars, to find their central positions on the assumption that those objects have a symmetric distribution concentrated at the center of the Galaxy (Shapley 1918). The second is to observe water masers or massive objects in the Galactic central region to yield the distance to this region via the kinematical data. The other way is based on the radial-velocity data of stars of the thin-disk population, e.g. Galactic Cepheids, to constrain the local kinematical parameters in the solar vicinity.

Encouraged by our above kinematical analysis, in which we find that the Oort constant A is independent of the cluster age, we decided to design a further investigation to derive the Galactocentric distance of the Sun R_0. Because only small values C and K of the Oort constants are found in the last section, we are able to simply use an axisymmetric rotation model. The Oort constant A is independently derived from proper motions of clusters, then we apply this constant to constrain the kinematical model from the radial velocities

$$\begin{aligned} v_r &= 2AR_0(\frac{R_0}{R} - 1)\sin\ell\cos b \\ &\quad -U_\odot \cos\ell\cos b - V_\odot \sin\ell\cos b - W_\odot \sin b - \delta v_r, \end{aligned} \tag{11}$$

$$R = (R_0^2 + r^2\cos^2 b - 2R_0 r\cos\ell\cos b)^{\frac{1}{2}}. \tag{12}$$

In the above equations, δv_r is a possible offset of the zero point of the radial-velocity system. R is the Galactocentric radius of a cluster.

Using 269 clusters as selected in the above section, we derive the Oort constants A and B from proper motions of clusters, based on an axisymmetric kinematical model. The corresponding parameters are listed in Table 6. Then, applying the least-squares to Equation (11), the parameter $2AR_0$ can be obtained from the radial velocities. Taking a constant A from the proper-motion solution, the Galactocentric distance R_0 will be obtained. Table 6 shows all kinematical parameters, including the Galactocentric distance of the Sun, separately determined from the proper motions and radial velocities of the selected clusters. The final solution of R_0 is obtained in an iterative way.

Note that $W_\odot$ is impossible to derive from Equation (11) because of the low scale height of the disk. On the other hand, the component of the solar motion $W_\odot$ is not correlated with the other parameters in Equation (11). Thus, we can favorably fix $W_\odot = 7.2$ km s^{-1}, according to the measurement by Dehnen & Binney (1998).

The present determination of R_0 is based on independent observations for proper motions and radial velocities of clusters. It gives $R_0 = 8.03 \pm 0.70$ kpc that is consistent with the current 'best estimate' of $R_0 = 8.0 \pm 0.5$ kpc proposed by Reid (1993). For comparison, we list individual determinations of R_0 in Table 7, given by different authors with various observations and methods published in the last decades.

6 DISCUSSION ABOUT ROTATION CURVE

According to the Oort constants derived from all clusters (Table 5), which are based on the proper-motion and radial-velocity analysis of all age clusters, we obtain the circular speed of the Galactic rotation $V_0 = 235 \pm 10$ km s^{-1}, supposing $R_0 = 8$ kpc. This value is almost identical with the rotational

Table 6 Galactocentric distance of the Sun and other kinematical parameters obtained from open clusters. The unit is in $\mathrm{km\,s^{-1}}$ for δv_r, $2AR_0$, and solar-motion components. The Oort constants are measured in $\mathrm{km\,s^{-1}\,kpc^{-1}}$. R_0 is in kpc.

Data	$U_\odot$	$V_\odot$	$W_\odot$	A	B	$2AR_0$	δvr	R_0
Proper motions	10.82	11.41	7.75	16.16	−13.19			
	±0.69	±0.70	±0.52	±1.07	±0.76			
Radial velocities	9.92	12.34	7.20	16.16		259.5	2.42	8.03
	±1.24	±1.18	(set)	(set)		±14.7	±0.86	±0.70

Table 7 Calibrations of R_0 Given by Individual Investigators with Different Observations and Methods

Authors	Observation & Method	R_0 (kpc)
Kerr & Lynden-Bell (1986)	1985 IAU recommendation	8.5±0.5
Caldwell & Coulson (1987)	Cepheid radial velocities	7.8±0.7
Racine & Harris (1989)	globular clusters	7.5±0.9
Dopita et al. (1992)	planetary nebulae in the Galactic bulge	7.6±0.7
Pont et al. (1994)	Cepheid radial velocities	8.09±0.30
Carney et al. (1995)	RR Lyraes	7.8±0.4
Feast & Whitelock (1997)	R_0 from Pont et al. corrected with a new PL relation	8.5±0.5
Metzger et al. (1998)	Cepheid radial velocities	7.66±0.32
Genzel et al. (2000)	stars around the center region of the Galaxy	7.8∼8.2 ±0.9
Eisenhauer et al. (2003)	orbit of star S2 around the Galactic center	7.94±0.42
Bica et al. (2006)	globular clusters	7.2±0.3
Reid (1993)	'best value' from statistical average	8.0±0.5
this paper	from μ_b of Sgr A* given by Reid & Brunthaler (2004)	7.49±0.86
this paper	proper motions and radial velocities of open clusters	8.03± 0.70

velocity of the Galaxy derived from the proper-motion analysis (Table 6) and is a little faster than the 1985 IAU recommended value of $V_0 = 220\,\mathrm{km\,s^{-1}}$ (Kerr & Lynden-Bell 1986). Using the tangential and radial velocities of clusters, and accepting $V_0 = 220\,\mathrm{km\,s^{-1}}$ and $R_0 = 8\,\mathrm{kpc}$, the rotation curve defined by the open clusters within a range less than 3.0 kpc near the Sun can be constructed.

The top panel of Figure 9 illustrates the variation of the circular speed as a function of the Galactocentric distance R. The schematic structure of the curve is similar to those given by many other investigators, e.g. by Avedisova (2005), who fit the rotation curve based on the observation data of the Galactic CO molecular gas. The average slope of the decline of the rotation curve is $-4.6 \pm 0.8\,\mathrm{km\,s^{-1}\,kpc^{-1}}$, which is even steeper than those given by Oort constants $(-A - B)$ derived from all clusters in Tables 5 and 6. This difference is easily understood from the figure, because $(-A - B)$ gives the radial variation of the rotation speed at the Sun, and the slope at $R = R_0$ is nearly flat.

The persistence of a significant K-term or v_r in radial velocities for Galactic young objects has been recognized for a long time (Feast 1967; Humphreys 1972), which can be explained either as an overall kinematical contraction or an expansion of the Galactic plane, or as a systematic error in measuring the radial velocities. On the other hand, if an axisymmetric model is not sufficient to describe the Galactic rotation defined by the young disk stars, say, the young objects are along the oval orbits on the Galactic plane, a non-axisymmetric model should be introduced to describe their kinematical behaviors. Considering rotation velocities of clusters as functions of the azimuthal angle (the bottom panel of Fig. 9), we find that the circular speed gradually decreases in the direction of the Galactic rotation. This fact might be evidence for the open clusters moving on oval orbits rather than on circular orbits. The non-circular motions of clusters may be driven by the weak Galactic bar. Based on the simple model of an elliptical disk given by Kuijken & Tremaine (1994), we have found a clear weak elliptical potential of the disk with an ellipticity of $\epsilon(R_0) = 0.060 \pm 0.012$ (Zhu 2008); the motion of clusters is suggested to be on an oval orbit other than circular rotation.
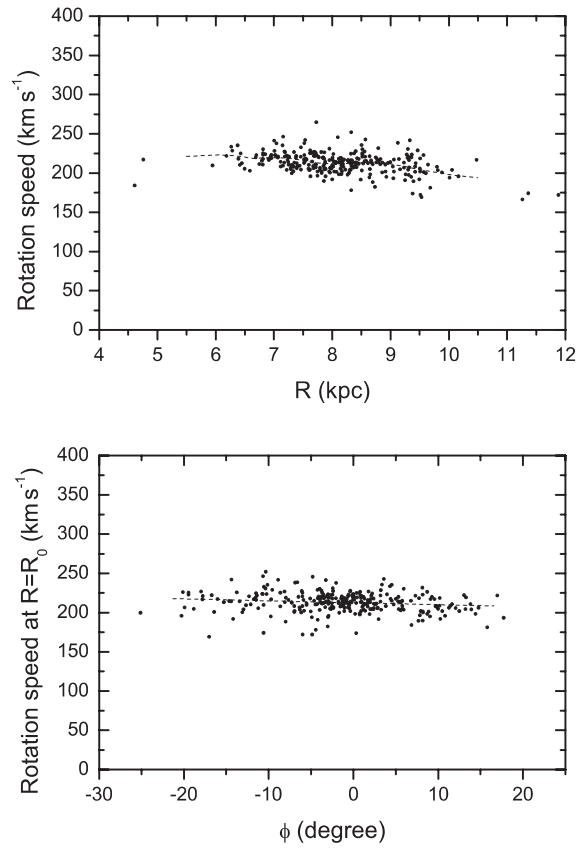
Fig. 9 Rotation curve defined by open clusters, supposing $V_0 = 220 \, \text{km s}^{-1}$ and $R_0 = 8 \, \text{kpc}$. The top panel shows the circular speeds against the Galactocentric distances of clusters, the bottom panel gives their variations as functions of their Galactocentric azimuthal angle from the Sun.

7 SUMMARY

On the basis of proper motions, radial velocities, heliocentric distances, and ages of about 300 open clusters within a range of $r \leq 3.0 \, \text{kpc}$ from the Sun, we have determined the vertical distribution of the Galactic thin-disk. We obtain the mean scale height of the disk and the vertical displacement of the Galactic plane

$$z_{\text{h}} = 58 \pm 4 \, \text{pc} ,$$
$$z_0 = -16 \pm 4 \, \text{pc} ,$$

that are derived from all clusters of all ages. Clusters with ages younger than 50 Myr have a thin scale-height of $z_{\text{h}} = 51 \pm 5 \, \text{pc}$, whereas a clearly increased scale-height of $z_{\text{h}} = 67 \pm 6 \, \text{pc}$ for clusters older than 50 Myr is found.

From the kinematical analysis, we find that clusters seem to exhibit a constant shear motion about the Galactic center, while the vorticity of their motion becomes slower with the increase of their ages. The Oort constants are given for all clusters of all ages:

$$A = 16.44 \pm 0.94 \, \text{km s}^{-1} \, \text{kpc}^{-1} ,$$
$$B = -12.91 \pm 0.89 \, \text{km s}^{-1} \, \text{kpc}^{-1} .$$

The total solar motion with the apex towards $\ell_\odot$ and $b_\odot$ is as follows:

$$S = 19.5 \pm 0.6 \text{ km s}^{-1},$$
$$\ell_\odot = 48.6° \pm 1.9°,$$
$$b_\odot = 24.5° \pm 1.6°.$$

Using the observational data of clusters, we are able to determine the Oort constants independently from the proper motions. As a constraint, the Oort constant A is applied to derive the Galactocentric distance of the Sun via the radial velocity data. We yield $R_0 = 8.03 \pm 0.70$ kpc, which is firmly consistent with the best estimate of R_0 suggested by Reid (1993). The circular speed of the Galactic rotation is then obtained as $V_0 = 235 \pm 10$ km s^{-1} for all clusters of all ages.

References

Avedisova, V. S. 2005, Astronomy Reports, 49, 435

Bica, E., Bonatto, C., Barbuy, B., & Ortolani, S. 2006, A&A, 450, 105

Bonatto, C., Kerber, L. O., Bica, E., & Santiago, B. X. 2006, A&A, 446, 121

Caldwell, J. A. R., & Coulson, I. M. 1987, AJ, 93, 1090

Carney, B. W., et al. 1995, AJ, 110, 1674

Chen, B., Stoughton, C., Smith, J. A., et al. 2001, ApJ, 553, 184

Dehnen, W., & Binney, J. J. 1998, MNRAS, 298, 387

Dias, W. S., Alessi, B. S., Moitinho, A., & Lépine, J. R. D. 2002, A&A, 389, 871 (DAML02)

Dias, W. S., & Lépine, J. R. D. 2005, AJ, 629, 825

Dias, W. S., Lépine, J. R. D., Bruno, S. A., & Moitinho, A. 2006, Open clusters and Galactic structure,
   http://www.astro.iag.usp.br/~wilton/

Dias, W. S., Alessi, B. S., Moitinho, A., & Lépine, J. R. D. 2008, Optically visible open clusters and candidates,
   http://cdsarc.u-strasbg.fr/viz-bin/Cat?B/ocl

Dopita, M. A., Jacopy, G. H., & Vassiliadis, E. 1992, ApJ, 389, 27

Eisenhauer, F., et al. 2003, ApJ, 597, L121

Feast, M. W. 1967, MNRAS, 136,141

Feast, M. W., & Whitelock, P. 1997, MNRAS, 291, 683

Genzel, R., et al. 2000, MNRAS, 317, 348

Humphreys, R. M. 1972, A&A, 20, 29

Kaempf, T. A., de Boer, K. S., & Altmann, M. 2005, A&A, 432, 879

Kerr, F. J., & Lynden-Bell, D. 1986, MNRAS, 221, 1023

Kharchenko, N. V. 2001, Kinematics and Physics of Celestial Bodies, 17, 409

Kharchenko, N. V., Piskunov, A. E., Röser, S., Schilbach, E., & Scholz, R. D. 2005a, A&A, 438, 1163

Kharchenko, N. V., Piskunov, A. E., Röser, S., Schilbach, E., & Scholz, R. D. 2005b, A&A, 440, 403

Kharchenko, N. V., Scholz, R. D., Piskunov, A. E., Röser, S., & Schilbach, E. 2007, Astron. Nachr., 328, 889

Kuijken, K., & Tremaine, S. 1994, ApJ, 421, 178

Lindblad, P. O. 2000, A&A, 363, 154

Lyngå, G. 1987, Open Cluster Data, 5th Edition (Strasbourg: CDS, VII/92A)

Méndez, R. A., Platais, I., Girard, T. M., et al. 1999, ApJ, 524, L39

Méndez, R. A., Platais, I., Girard, T. M., et al. 2000, AJ, 119, 813

Metzger, M. R., Caldwell, J. A. R., & Schechter, P. L. 1998, AJ, 115, 635

Miyamoto, M., & Zhu, Z. 1998, AJ, 115, 1483

Olano, C. A. 1982, A&A, 112, 195

Olling, R. P., & Dehnen, W. 2003, ApJ, 599, 275

Oort, J. H. 1932, Bull. Astron. Inst. Netherlands, 6, 249

Paunzen, E., & Netopil, M. 2006, MNRAS, 371, 1641

Piskunov, A. E., Kharchenko N. V., Röser, S., Schilbach, E., & Scholz, R. D. 2006, A&A, 445, 545

Pont, F., Mayor, M., & Burki, G. 1994, A&A, 285, 415

Racine, R., & Harris, W. E. 1989, AJ, 98, 1609

Reid, M. J. 1993, ARA&A, 31, 345

Reid, M. J., & Brunthaler, A. 2004, ApJ, 616, 872

Spagna, A., Bucciarelli, B., Carollo, D., et al. 2005, in The Three-Dimensional Universe with Gaia, eds. C. Turon,
    K. S. O'Flaherty, & M. A. C. (Perryman: ESA) SP-576, 193

Shapley, H. 1918, ApJ, 48, 154

Torra, J., Fernández, D., & Figueras, F. 2000, A&A, 359, 82

Westin, T. N. G. 1985, A&AS, 60, 99

Zhu, Z. 2000, Ap&SS, 271, 353

Zhu, Z. 2008, ChJAA (Chin. J. Astron. Astrophys.), 8, 96